Transactions of the Materials Research Society of Japan 31[4] 895-898 (2006)

Influence of nano-structural feature in M_2O_3 doped CeO_2 (M=Sm, Y, Yb) solid electrolytes on oxide ionic conductivity for fuel cell applications

Toshiyuki Mori, Ding-Rong Ou, Fei Ye,
Yarong WANG and John Drennan*
Nation Institute for Materials Science,
1-1 Namiki, Tsukuba, Ibaraki, 305-0044, Japan
Fax: 81029-860-4667, Mori.Toshiyuki@nims.go.jp
*The University of Queensland
St.Lucia, Brisbane, Qld 4072 Australia

Doped ceria (CeO_2) compounds are fluorite type oxides, which show oxide ion conductivity higher than yttria stabilized zirconia, in oxidizing atmospheres. As a consequence of this, considerable interest has been shown in application of these materials for 'low (400°- 600°C)' temperature operation of solid oxide fuel cells (SOFCs). In this study, some rare earth (ex. Sm, Y, and Yb) doped CeO_2 nano-powders were synthesized via a carbonate co-precipitation method. Fluorite type solid solution was formed at low temperature such as 400°C and the dense sintered bodies were fabricated in the temperature ranging from 1000° to 1450°C by conventional sintering (CS) method. To develop the high quality solid electrolytes, the microstructures in doped CeO_2 solid electrolytes were examined using transmission electron microscopy. The sintered specimens had continuous and large micro-domains with distorted pyrochlore structure or distorted c-type rare earth structure in the grain. It is concluded that the conducting properties in the doped CeO_2 was strongly influenced by size of micro-domain in the grain. It is found that the domain size in the sintered bodies can be minimized using round shaped doped CeO_2 powders. Therefore, we believe that domain size control will be a key for development of high quality doped CeO_2 solid electrolytes.

Key words: doped CeO_2, micro-domain, oxide ion conduction, solid electrolyte, solid oxide fuel cell

1. INTRODUCTION

Oxide ion conductors are used in a variety of gas sensors,[1,2] solid oxide electrochemical cells (SOECs),[3,4] and solid oxide fuel cells (SOFCs).[5,6] In these applications, SOFCs are being especially developed as a clean and efficient power source for generating electricity from a variety of fuels. For systems that have long lifetimes and which operate at low temperatures (400° - 600°C) efficiently, it is necessary to produce materials with high oxide ion conduction for application as electrolytes in all of these systems. Yttria stabilized zirconia (YSZ) and scandia stabilized zirconia (SSZ) are common electrolytes used in SOFCs. However, their respective ionic conductivities do not allow for low temperature operation of SOFCs. Accordingly, it is important that a high-quality electrolyte materials with higher oxide ion conductivity than that of YSZ and SSZ be identified – the systems based on CeO_2 fit this demand.

Trivalent metal oxides such as rare earth oxide doped CeO_2 possess higher oxide ion conductivity than aforementioned stabilized zirconia systems. [7] At high oxygen partial pressures, these doped CeO_2 electrolytes show high oxide ion conductivity, however at low oxygen partial pressures, associated with anodic conditions in fuel cell systems, the Ce^{4+} ion can be partially reduced to Ce^{3+} ion. In this reduction of CeO_2 based oxides, quasi-free electrons are introduced into a fluorite lattice and the consequent increase in electronic conductivity reduces the efficiency of the cell. The stability in both oxidizing and reducing atmosphere is an essential requirement for candidate electrolytes materials and although the rare earth doped CeO_2 systems show considerable promise, attention must be paid to overcoming this difficulty of operating in the reducing conditions of the anodic part of the cell. Apart from protecting the surface of the electrolyte with less susceptible materials, the possibility exists that by successfully designing the microstructure of the electrolyte material at the nano-scale, it will be possible to minimize the effects of reduction in low temperature SOFCs. This effective re-design at the nano-scale will lead to an enhanced conduction pathway producing materials less susceptible to electronic conduction. As a consequence, the control of the processing parameters to produce the desired microstructure will be an essential part of the development of materials with designed nano-structures.

In this paper, the influence of microstructure at

the atomic level of dense specimens on conducting properties was examined with a view to finding new ways of improving the conducting properties of doped CeO_2.

2. EXPERIMENTAL

2.1 Powder synthesis and sintered body fabrication - The starting materials used for Sm doped CeO_2, Y doped CeO_2, and Yb doped CeO_2 synthesis were cerium nitrate hexahydrate ($Ce(NO_3)_3 \cdot 6H_2O$; >99.99% pure, KANTO Chemical Co. Inc., Japan), samarium nitrate hexahydrate ($Sm(NO_3)_3 \cdot 6H_2O$; >99.95% pure, KANTO Chemical Co. Inc., Japan), yttrium nitrate hexahydrate ($Y(NO_3)_3 \cdot 6H_2O$; >99.9% pure, Wako Pure Chemical Industries Inc., Japan), ytterbium nitrate hexahydrate ($Yb(NO_3)_3 \cdot 6H_2O$; >99.9% pure, Wako Pure Chemical Industries Inc., Japan) and ammonium carbonate ($(NH_4)_2CO_3$; Ultrahigh purity, KANTO chemical Co. Inc., Japan). The cerium nitrate hexahydrate and the relevant dopant nitrate hexahydrate powders were dissolved into distilled water, and the solutions were mixed in order to prepare the composition of $Sm_xCe_{1-x}O_{2-x/2}$, $Y_xCe_{1-x}O_{2-x/2}$ and $Yb_xCe_{1-x}O_{2-x/2}$ (x=0.1, 0.15, 0.2 and 0.25). An aqueous solution of ammonium carbonate in distilled water with a concentration of 1.5M was used as the precipitant. The mixed solution was added into the ammonium carbonate solution kept at 70°C whilst being gently stirred. After repeated washing, the precipitate was dried at room temperature in a nitrogen gas flow and then calcined in flowing oxygen at 700°C for 2h to yield the rare-earth doped powders. For sintering, these powders were initially molded at a pressure of 98MPa and then subjected to a further pressing using a rubber die at 390MPa in order to obtain a green body. Sintering temperature ranged from 1000° to 1450°C for 6h.

2.2 Sample characterization - The crystal phases in the powder and sintered specimens were investigated using X-ray diffraction analysis (XRD, monochromated CuKα, 50 KV, 25mA) and a selected area electron diffraction analysis, respectively. Simulated electron diffraction pattern was calculated using software *CaRIne* (CaRine Crystallography, version3.1 (presented by Boudias and Monceau (CaRine Crystallography, Senlis, France). The bulk density of the sintered body was measured using the Archimedes method. The relative density was calculated from the ratio of the measured bulk density to the theoretical density. The theoretical density was estimated using the lattice constant and the sample composition. The particle sizes in the synthesized powders were observed using scanning electron microscopy (SEM). The average grain size in the sintered body was calculated using the linear intercept method, measuring more than 300 grains recorded using micrographs produced by a SEM. The microstructural features in the grain were investigated in detail using transmission electron microscopy (TEM). TEM observation was performed with gun voltages of 200keV.

2.3 Measurement of electrical properties – Electrical conductivity of the sintered specimens was measured by dc three-point measurements at 400° - 650°C in air. A platinum electrode was applied to both sides of the sintered bodies at 1000°C for 1h in air. The dimensions of the specimens were 10mm in diameter and 2mm in thickness for the three-point measurements. The activation energy was calculated using the data of conductivity at the temperature ranging from 400° to 650°C.

3. RESULT AND DISCUSSION

Figure 1 presents SEM image of particle morphologies of calcined round shape particles of $Sm_{0.2}Ce_{0.8}O_{1.9}$. The round shaped particles were prepared when $(NH_4)_2CO_3/Sm^{3+}$ molar ratio was equal to 15. The calcinded particles were observed to be composed of uniformly sized, round, and discrete particles. The average particle size of calcined powders was approximately 30nm. The morphology and size of particles of other compositions (i.e. $Sm_xCe_{1-x}O_{2-x/2}$, x=0.1, 0.15 and 0.25) were as almost same as those of $Sm_{0.2}Ce_{0.8}O_{1.9}$. These powders can be sintered to over 95% dense of theoretical density in the temperature range of 1050° to 1450°C using conventional sintering method.

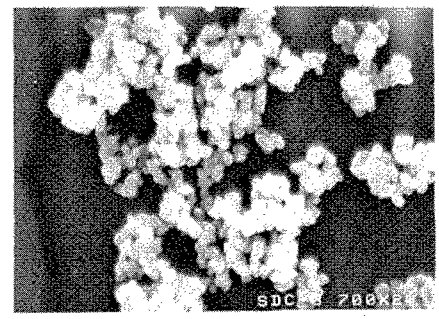

Fig.1 SEM image of nano-size round shaped particles of $Sm_{0.2}Ce_{0.8}O_{1.9}$. Calcination temperature: 700°C, calcination time:2h.

A combination of conducting properties and microstructure are shown for $Sm_xCe_{1-x}O_{2-x/2}$ (x=0.1, 0.15, 0.2 and 0.25) sintered bodies, in figure 2 (a) and (b). The activation energy of Sm doped CeO_2 electrolytes was minimized at the composition around x=0.15 in the $Sm_xCe_{1-x}O_{2-x/2}$ system. Also, the conductivity shows the maximum at the same composition indicating that the mobility of oxide ions is greatest at the aforementioned composition in this system. To throw some light on the reason for why the conductivity and activation energy are optimized at this value of doping, in Sm doped CeO_2, the crystal phases and associated nano-structural features in the sintered bodies were examined with a view to observing any correlations. The selected area electron diffraction patterns

(SAEDPs) recorded from $Sm_{0.1}Ce_{0.9}O_{1.95}$ and $Sm_{0.25}Ce_{0.75}O_{1.875}$ sintered bodies have extra reflections, and this is in contrast to the X-ray diffraction profiles recorded from these sintered bodies which indicate a simple fluorite phase. In addition to the extra reflections were observed regions of associated diffuse scattering and this phenomenon are common to both specimens. The intensity of extra reflection and diffuse scattering in SAEDP of $Sm_{0.25}Ce_{0.75}O_{1.875}$ is much stronger than that of $Sm_{0.1}Ce_{0.9}O_{1.95}$. This indicates that both specimens exhibit diffraction phenomenon consistent with the existence of micro-domains representing some coherent ordered structure associated with oxygen vacancies. The average micro-domain size in $Sm_{0.25}Ce_{0.75}O_{1.875}$ is larger than that observed in $Sm_{0.1}Ce_{0.9}O_{1.95}$. It is found that the distribution of the extra reflections and diffuse scattering is consistent with the occurrence of micro-domains with a distorted pyrochlore structure. We arrive at this conclusion by comparing observed SAEDPs with those calculated using pyrochlore data. From these observations we suggest that in materials in which the micro-domains are large, the conductivity is lowered.

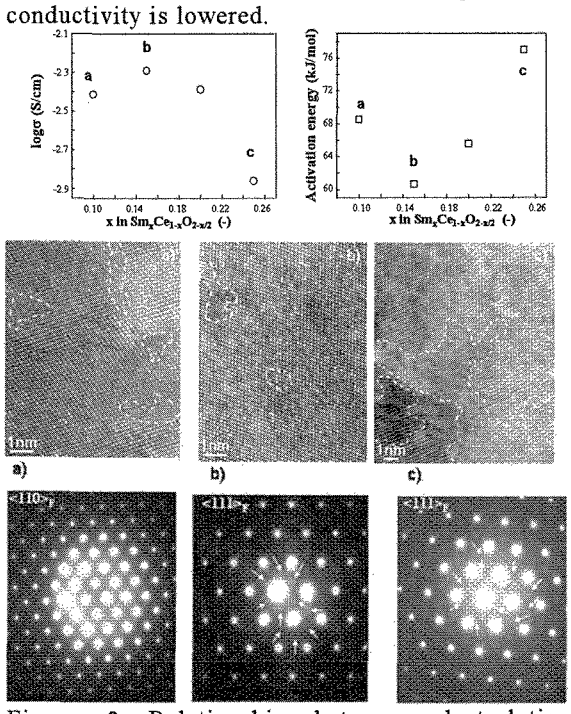

Figure 2 Relationship between electrolytic properties (conductivity and activation energy) and nano-structural features in $Sm_xCe_{1-x}O_{2-x/2}$ (x=0.1, 0.15, 0.2 and 0.25). Dashed line area in high resolution image is micro-main. The arrow symbol in SAEDPs indicates the extra-reflection. a: $Sm_{0.1}Ce_{0.9}O_{1.95}$, b: $Sm_{0.15}Ce_{0.85}O_{1.925}$, and c:$Sm_{0.25}Ce_{0.75}O_{1.875}$.

The relationship between the conducting properties and nano-structural features in Y doped CeO_2 and Yb doped CeO_2 follows the same pattern as that in Sm doped CeO_2 system. In the case of Y doped CeO_2 and Yb doped CeO_2, the micro-domains consist of distorted c-type rare earth structure.

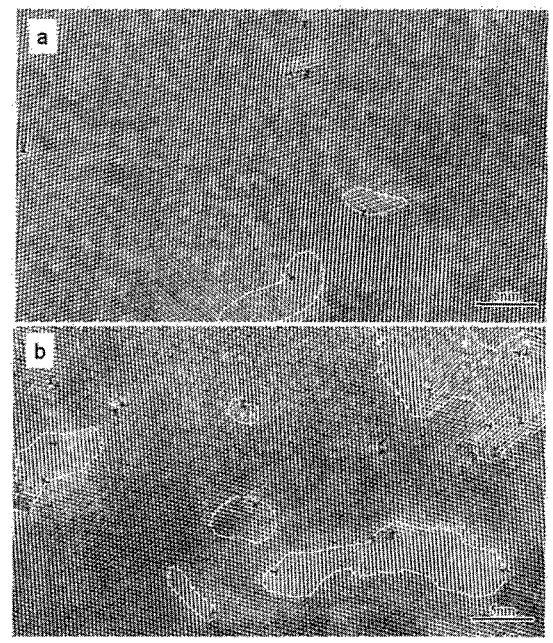

Figure 3 High resolution images recorded from a: $Y_{0.15}Ce_{0.85}O_{1.925}$, and b:$Y_{0.25}Ce_{0.75}O_{1.875}$. The dashed line area indicates the micro-domain.

The micro-domain size (approx. 5nm) in $Y_{0.15}Ce_{0.85}O_{1.925}$ with high conductivity was much smaller than that (5nm to 20nm) observed in $Y_{0.25}Ce_{0.75}O_{1.875}$ as shown in figure 3. This is consistent with the observations outlined in Fig.2 and observation results in Yb doped CeO_2 system. To characterize the micro-domain, we observed dopant concentration in micro-domain using TEM equipped with electron energy loss spectroscopy (EELS). The concentration of dopant in the domain was higher than that in the matrix. This suggests that segregation of dopant influences the formation of micro-domain in the specimen. Therefore, it is concluded that micro-domain size and conductivity are influenced by a processing route for fabrication of dense doped CeO_2 solid electrolytes.

To conclude the influence of processing route on the micro-domain size at atom level and conducting properties in doped CeO_2 solid electrolyte, nano-size elongated particles of $Sm_{0.2}Ce_{0.8}O_{1.9}$ were prepared. The elongated particles were obtained at $(NH_4)HCO_3/Sm^{3+}$ molar ratio = 25. The chemical composition of both round shaped particles and elongated particles was $Sm_{0.21}Ce_{0.79}O_{1.89}$. The composition of powders was controlled well with very small deviation. Figure 4 shows temperature dependence of electrical conductivity of the $Sm_{0.2}Ce_{0.8}O_{1.9}$ sintered bodies made from nano-size round shape particles and nano-size elongated particles. The relative density of both specimens reaches 95% of the theoretical. The conductivity of sintered body made from round shape particles was higher than that of sintered body made from elongated particles over the

entire measurement temperature region. The activation energy of the specimen made from round shape particles and the specimen made from elongated particles was 65 and 74kJ/mol, respectively. On the other hand, the activation energy of the previous reported $Sm_{0.2}Ce_{0.8}O_{1.9}$ is 75.2 kJ/mol.[8] The activation energy of previous reported $Sm_{0.2}Ce_{0.8}O_{1.9}$ almost agrees with that of specimen made from elongated particles in the present study. The activation energy of specimen made from round shape particles presented in Fig.4 was much lower than that of the similar system cited previously.

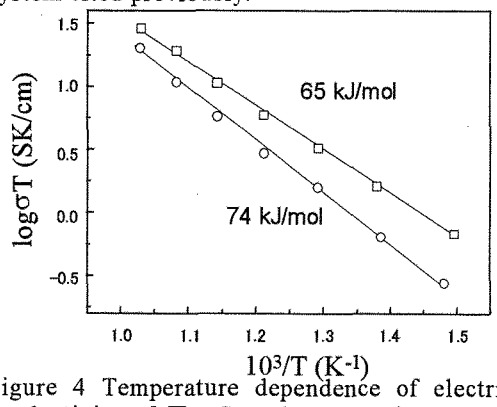

Figure 4 Temperature dependence of electrical conductivity of □ : $Sm_{0.2}Ce_{0.8}O_{1.9}$ sintered body made from round shape particles, and O : $Sm_{0.2}Ce_{0.8}O_{1.9}$ sintered body made from elongated particles.

To conclude the influence of microstructure on conducting properties in Fig.4, the micro-structural feature was observed using TEM. The extra reflection and diffuse scattering in electron diffraction patterns recorded from both specimens were observed. The micro-domain size in $Sm_{0.2}Ce_{0.8}O_{1.9}$ specimen made from round shape particles (approximately 2nm) was smaller than that (approximately 10nm) in $Sm_{0.2}Ce_{0.8}O_{1.9}$ specimen made from elongated particles. This indicates that the segregation of dopant in the sintered bodies is enhanced using nano-size elongated particles. The conducting properties in the specimen made from elongated particles were lowered using elongated particles. Accordingly, it is concluded that a control of processing route is a key to minimize the micro-domain size and maximize the conducting properties in doped CeO_2 solid electrolytes.

4. CONCLUSION

Nano-crystalline doped CeO_2 powders were synthesized using carbonate co-precipitation method. Also the influence of the produced nano-structural features in the specimens on the conducting properties of the ceramics was examined. In general, the tri-valent cations are known to replace Ce^{4+} and create oxygen vacancies. It is also known that segregation of dopant cations in the specimen occurs. This would induce a localized lattice expansion in the grain. To minimize the lattice distortion in CeO_2 lattice, micro-domains would form with ordered structure of oxygen vacancies, even though segregation level is subtle. The micro-domains with distorted pylochlore or c-type rare structure were observed in the doped CeO_2 solid electrolytes. The larger micro-domains would necessarily contain a greater number of ordered vacancies which effectively removes them from being potential oxygen transport sites. As a consequence of this, a material with larger micro-domains lowers the conductivity in the specimens. The author believes that the micro-domain size should be minimized in the specimens to improve the conducting properties in doped CeO_2 solid electrolytes. In the present study, the influence of particle morphology of doped CeO_2 powders on micro-domain size and conducting properties in doped CeO_2 solid electrolytes. Since the difference of particle morphology influences the conducting properties and micro-domain size in the doped CeO_2 sintered body, a control of sintering behavior of specimen using easy-sinterable powders is an important parameter for the design of nano-structures in doped CeO_2 solid electrolytes. And we believe that the design of nano-structure in doped CeO_2 using combined technique of the processing route control and nano-structure analysis is useful for improvement of conductivity in doped CeO_2 solid electrolytes.

REFERENCES

[1] N.Yamazoe and N.Miura, "Gas sensors using solid electrolytes", *MRS Bull.*, **24**(6), 37-43(1999).
[2]M.Nakatou and N.Miura, "Impedance-metric sensor based on YSZ and In_2O_3 for detection of low concentrations of water vapor at high temperature", *Electrochemistry Communications*, **6** (10): 995-998(2004).
[3]S.Hamakawa, T.Hayakawa, A.P.K.York, T.Tsunoda, Y.S.Yoon, K.Suzuki, M.Shimizu and K.Takehira, "Selective oxidation of propene using an electrochemical membrane reactor with CeO_2 based solid electrolyte", *J.Electrochem.Soc.*, **143**(4), 1264-1268(1996).
[4]S.Hamakawa, T.Hayakawa, K.Suzuki, K.Murata, K.Takehira, S.Yoshino, J.Nakamura and T.Uchijima, "Methane conversion into synthesis gas using an electrochemical membrane reactor", *Solid State Ionics*, **136**, 761-766(2000).
[5]N.Q.Minh, "Ceramic fuel cells", *J.Am.Ceram.Soc.*, **76**(3), 563-588(1993).
[6]B.C.H.Steel, "Materials for fuel-cell technologies", *Nature*, **414**(15), 345-352(2001).
[7] J.Kilner, "Fast oxygen transport in acceptor doped oxides", *Solid State Ionics*, **129**, 13-23(2000).
[8] R. T. Dirstine, R. N. Blumenthal, and T. F. Kuech, "Ionic-conductivity of calcia, yttria, and rare earth doped cerium dioxide", *J. Electrochem. Soc.*, **126** [2] 264-269(1979).

(Received December 11, 2005;Accepted September 1, 2006)